Affibody-mediated imaging of EGFR expression in prostate cancer using radiocobalt-labeled DOTA-$Z_{EGFR:2377}$

BOGDAN MITRAN[1*], KEN GÖSTA ANDERSSON[2*], ELIN LINDSTRÖM[1], JAVAD GAROUSI[3], MARIA ROSESTEDT[1], VLADIMIR TOLMACHEV[3], STEFAN STÅHL[2], ANNA ORLOVA[1,4*] and JOHN LÖFBLOM[2*]

[1]Department of Medicinal Chemistry, Uppsala University, SE-751 83 Uppsala; [2]Department of Protein Science, School of Engineering Sciences in Chemistry, Biotechnology and Health, KTH Royal Institute of Technology, SE-106 91 Stockholm; [3]Department of Immunology, Genetics and Pathology, Uppsala University, SE-752 85 Uppsala; [4]Science for Life Laboratory, Department of Immunology, Genetics and Pathology, Uppsala University, SE-751 08 Uppsala, Sweden

Received November 10, 2017; Accepted September 20, 2018

DOI: 10.3892/or.2018.6792

Abstract. The epidermal growth factor receptor (EGFR) is often overexpressed during prostate cancer (PCa) progression towards androgen-independence after hormone therapy, but the overexpression is lower than in other types of cancers. Despite the low expression, EGFR has emerged as a promising therapeutic target for patients with castration-resistant PCa. Non-invasive methods for determination of EGFR expression in PCa can serve for patient stratification and therapy response monitoring. Radionuclide imaging probes based on affibody molecules (7 kDa) provide high contrast imaging of cancer-associated molecular targets. We hypothesized that the anti-EGFR affibody molecule DOTA-$Z_{EGFR:2377}$ labeled with ^{55}Co (positron-emitter, T1/2=17.5 h) would enable imaging of EGFR expression in PCa xenografts. The human PCa cell line DU-145 was used for *in vitro* and *in vivo* experiments and ^{57}Co was used as a surrogate for ^{55}Co in the present study. Binding of ^{57}Co-DOTA-$Z_{EGFR:2377}$ to EGFR-expressing xenografts was saturable with anti-EGFR monoclonal antibody cetuximab, which would motivate the use of this tracer for monitoring the receptor occupancy during treatment. A significant dose-dependent difference in radioactivity accumulation in tumors and normal organs was observed when the biodistribution was studied 3 h after the injection of 10 and 35 μg of ^{57}Co-DOTA-$Z_{EGFR:2377}$: At lower doses the tumor uptake was 2-fold higher although tumor-to-organ ratios were not altered. For clinically relevant organs for PCa, tumor-to-organ ratios increased with time, and at 24 h pi were 2.2±0.5 for colon, 7±2 for muscle, and 4.0±0.7 for bones. Small animal SPECT/CT images confirmed the capacity of radiocobalt labeled DOTA-$Z_{EGFR:2377}$ to visualize EGFR expression in PCa. In conclusion, the present study demonstrated the feasibility of using the radiocobalt labeled anti-EGFR affibody conjugate $Z_{EGFR:2377}$ as an imaging agent for *in vivo* visualization of low EGFR-expressing tumors, like PCa, and for monitoring of receptor occupancy during cetuximab therapy as well as the importance of optimal dosing in order to achieve higher sensitivity molecular imaging.

Correspondence to: Dr Anna Orlova, Department of Medicinal Chemistry, Uppsala University, Dag Hammarskjöldsv 14C, SE-751 83 Uppsala, Sweden
E-mail: anna.orlova@ilk.uu.se

*Contributed equally

Key words: prostate cancer, molecular imaging, cobalt, affibody molecule, HER1, EGFR

Introduction

Prostate cancer (PCa) growth is primarily driven by androgens (1). Therefore, androgen deprivation therapy (ADT), accomplished by surgical or medical castration, is the first-line therapeutic approach for the treatment of oligometastatic or high-risk localized PCa. ADT generally leads to remissions that last 1.5-3 years (2). However, despite the high initial response rate (3), the cancer almost invariably relapses, progressing to a hormone refractory state manifested by increased proliferation and invasion capacity. Hormone-refractory PCa is unresponsive to further hormonal manipulation and has a high resistance to cytotoxic drugs (4,5).

Although the molecular basis for such relapse is not fully defined, several signaling pathways have been identified by which androgen receptors are activated in the absence of ligands. Understanding these pathways is highly important for the development of new strategies for second-line therapies. One known mechanism responsible for androgen-independent growth involves alterations of growth factor receptor signaling (6,7). In particular, the epidermal growth factor receptor (EGFR) is one of the frequently deregulated gene products, and EGFR overexpression is associated with advanced stage PCa, progression towards androgen-independence and a poor clinical outcome (8-10).

EGFR, also known as ErbB1 or HER1, is a member of the tyrosine kinase EGFR family of receptors that also includes HER2/c-neu, HER3 and HER4. EGFR is activated by binding of specific ligands (EGF and TGFα are the preferred ligands), and three additional ligands that it shares with HER3 (11).

Recently, the role of EGFR in cancer is a subject of extensive investigations. Ligand binding to EGFR triggers its dimerization or heterodimerization with other members of the EGFR family and activates the intracellular tyrosine kinase domain. This further recruits downstream signaling proteins and triggers several signaling cascades that regulate growth, survival, proliferation, motility and differentiation (12). The understanding of these mechanisms has resulted in the development of drugs targeting EGFR and its signaling.

For patients, a confirmed EGFR overexpression in PCa could reveal new second line-treatment options involving monoclonal antibodies (mAb) such as the already established cetuximab (Erbitux®) (13,14) and small molecule tyrosine kinase inhibitors (TKIs) such as erlotinib (Tarceva®) (15,16) or gefitinib (Iressa®) (17,18). Many other new targeting drugs are also in preclinical and clinical development, either specifically targeting EGFR, or targeting several intracellular signaling pathways simultaneously (19). All these approaches are highly selective and the successful implementation of anti-EGFR therapies requires an accurate detection of EGFR expression in primary tumors and metastasis.

Currently, the most common and established method for the detection of EGFR expression involves analyses of biopsy material. However, biopsy procedures are invasive, painful, and can lead to severe complications. Repetitive biopsies and biopsies from bone metastases are difficult. Additionally, EGFR expression in PCa is a relatively late event and the target expression heterogeneity can lead to false-negative results. EGFR expression may also change during the course of the disease due to the genetic instability of the cancer or in response to treatment (20). There is a clear unmet clinical need for non-invasive robust methods to determine EGFR expression status, both initially and as a consequence of treatment.

Imaging of EGFR aberrant expression in PCa using radiolabeled EGFR-specific agents is a promising approach that allows repetitive, non-invasive investigations of receptor status in multiple lesions simultaneously. Potential radioimaging agents include the natural ligands of EGFR and the anti-EGFR mAbs. The use of radiolabeled epidermal growth factor (EGF) is a straightforward approach, but is limited by its physiological activity that may cause adverse reactions (nausea, vomiting, diarrhea, hypotension, fever and chills) (21). Radiolabeled intact anti-EGFR mAbs have been extensively investigated (22-28) demonstrating their capacity to specifically accumulate in tumors proportionally to EGFR expression. However, the sensitivity of mAb-mediated imaging is limited by the long blood residence time and slow tumor penetration, which reduces the imaging contrast, a major limitation for targets with low expression. A smaller targeting agent without physiological activity would be desirable in order to obtain a higher contrast than antibodies can provide.

Affibody molecules are a promising class of imaging agents that are characterized by small size and high affinity to the intended target. They are scaffold proteins composed of anti-parallel three-helix cysteine-free bundles, derived from the immunoglobulin-binding B domain of staphylococcal protein A. Randomization of 13 surface-exposed amino acids on helices 1 and 2 are used for generation of large combinatorial libraries from which high affinity binders can be selected. The small size (7 kDa) of affibody molecules facilitates rapid extravasation, rapid tumor penetration and fast clearance of unbound tracer from blood. This results in high contrast imaging only a few hours after injection, as seen in both preclinical and clinical studies (29-31).

Nonetheless, imaging of EGFR in PCa is challenging due to the relatively low expression in PCa (in comparison to other cancers). The feasibility of affibody-mediated imaging of EGFR expression was previously demonstrated using DOTA-$Z_{EGFR:2377}$. This construct was initially radiolabeled with ^{111}In, exhibiting favorable pharmacokinetic properties, with higher tumor-to-organ ratios than any anti-EGFR monoclonal antibody (32). In a further attempt to improve the sensitivity of EGFR detection *in vivo*, the use of positron-emitting labels was considered. Positron emission tomography (PET) provides better spatial resolution, higher sensitivity and more accurate quantification compared to single-photon emission computed tomography (SPECT). Several imaging probes based on $Z_{EGFR:2377}$ for PET imaging of EGFR were proposed for labeling with ^{68}Ga, ^{55}Co, and ^{89}Zr (33,34). Among them, the radiocobalt labeled affibody molecule had the most favorable biodistribution when evaluated on an epidermoid carcinoma model, A-431, with high EGFR-expression [$2x10^6$ receptors/cell (35)]. In this tumor model, radiocobalt labeled $Z_{EGFR:2377}$ demonstrated 2-fold higher tumor-to-blood, tumor-to-bone and tumor-to-muscle ratios compared to the same construct radiolabeled with ^{68}Ga and five-fold higher compared to ^{89}Zr-DFO-$Z_{EGFR:2377}$ at 3 h post injection (pi) (33,34).

The promising results obtained during the initial validation of radiocobalt-labeled DOTA-$Z_{EGFR:2377}$ in epidermoid carcinoma, provided the incentive for its evaluation in a more challenging, low receptor-expressing PCa model. In PCa, the high tumor-to-blood, tumor-to-bone and tumor-to-muscle ratios are particularly important, since the majority of metastases occur in the abdominal lymph nodes and bones. Moreover, the significantly lower liver uptake of ^{57}Co-DOTA-$Z_{EGFR:2377}$ compared to the ^{68}Ga-labeled analogue could be particularly relevant in a low EGFR-expressing tumors where protein dosing is crucial, as more injected compound would be available for specific binding to EGFR-expressing tumors and tissues.

The aim of the present study was to test the hypothesis that radiocobalt-labeled $Z_{EGFR:2377}$ affibody molecule would enable PET imaging of EGFR receptor expression in PCa xenografts where EGFR expression is low. A long-lived PET radionuclide, ^{55}Co has a half-life of 17.5 h, and would allow imaging the next day after injection when better contrast could be achieved (32). Cobalt-55 is not commercially available, which is an obstacle for pre-clinical investigations. However, we have recently demonstrated that data obtained for a bombesin analogue labeled with cobalt-57 ($T_{½}$=272 d) were fully translatable to cobalt-55 (36). Therefore, ^{57}Co was chosen as a surrogate for ^{55}Co in the present study.

Materials and methods

Labeling of DOTA-$Z_{EGFR:2377}$ with cobalt-57. The C-terminal cysteine-containing anti-EGFR affibody molecule Z_{2377}, conjugated with maleimido-derivative of DOTA, was produced as previously reported (32). Buffers for labeling were purified from metal contamination using Chelex 100 resin (Bio-Rad Laboratories, Inc., Richmond, CA, USA). Labeling with

radiocobalt and quality control methods were performed as previously described (33). Briefly, DOTA-$Z_{EGFR:2377}$ (50 μg) in 40 μl of 0.2 M ammonium acetate buffer, pH 5.5, was mixed with ^{57}Co stock solution (20 μl, 20-40 MBq). The reaction mixture was incubated for 30 min at 60˚C. After labeling, the conjugate was purified using disposable NAP-5 size-exclusion columns pre-equilibrated with phosphate-buffered saline (PBS). The yield and radiochemical purity of the conjugate were evaluated by instant thin-layer chromatography (ITLC) using Tec-Control Chromatography 150-771 strips (Biodex Medical Systems, Shirley, NY, USA) eluted with 0.2 M citric acid, pH 2.0. The distribution of radioactivity along the ITLC strips was measured on a Cyclone Storage Phosphor System (PerkinElmer, Inc., Waltham, MA, USA).

Cell culture. Human PCa cell line DU-145 [American Type Tissue Culture Collection (ATCC) via LGC Promochem, Borås, Sweden] was used. The EGFR expression in this cell line was ~2x10^5 receptors/cell (37). Roswell Park Memorial Institute medium (RPMI-1640) supplemented with 10% fetal calf serum (FCS), 2 mM L-glutamine and PEST (penicillin 100 IU/ml, streptomycin 100 μg/ml) (all from Biochrom AG, Berlin, Germany) was used for cell culturing. This medium was referred to as complete medium in the text. The cells were detached using a trypsin-EDTA solution (0.05% trypsin, 0.02% EDTA; Biochrom AG) and were counted using an electronic cell counter (Beckman Coulter, Inc., Brea, CA, USA).

In vitro cell studies. The *in vitro* binding specificity assay was designed to determine whether the binding of ^{57}Co-DOTA-$Z_{EGFR:2377}$ to EGFR-expressing DU-145 cells was receptor-mediated. In this experiment, the cells were incubated with 1 nM ^{57}Co-DOTA-$Z_{EGFR:2377}$ for 2 h at room temperature. One set of dishes was pre-incubated with i) 0.5 μM unlabeled affibody molecule, ii) one with 0.5 μM of cetuximab, and iii) one with 0.5 μM bevacizumab for 10 min at room temperature. After incubation with ^{57}Co-DOTA-$Z_{EGFR:2377}$, the cells were washed with serum-free media and detached using 0.5 ml trypsin-EDTA solution. The cell-associated radioactivity was assessed using a γ-counter (2480 WIZARD^2; PerkinElmer, Inc.) and presented as a percentage from added radioactivity.

Cellular processing was evaluated using DU-145 cells. The cells were incubated at 37˚C with 1.5 nM of ^{57}Co-DOTA-$Z_{EGFR:2377}$. At predetermined time-points (1, 2, 4, 8 and 24 h after the start of incubation) the membrane-bound and internalized radioactivity fractions were collected and calculated as previously described (37).

To assess the cellular retention of radioactivity after interrupted incubation with radiocobalt-labeled affibody molecules, cultured DU-145 cells were incubated for 1 h at 4˚C with 1.5 nM ^{57}Co-DOTA-$Z_{EGFR:2377}$. The cell dishes were subsequently washed with serum-free media, fresh complete media was added, and the dishes were incubated at 37˚C. At predetermined time-points, membrane-bound and internalized radioactivity fractions were collected and measured using the γ-counter.

The dissociation constant (K_D) of ^{57}Co-labeled DOTA-$Z_{EGFR:2377}$ binding to living DU-145 cells was measured using LigandTracer Yellow instruments (Ridgeview Instruments AB, Uppsala, Sweden) as previously described (38). Briefly, DU-145 cells were seeded in one area of the Petri dish (Nunclon™; 100-mm diameter; Thermo Fisher Scientific, Hvidovre, Denmark). After the addition of 3 ml of complete media, the dish was placed on the rotating table of the instrument. After a 15-min baseline run, ^{57}Co-labeled DOTA-$Z_{EGFR:2377}$ was added to the media to obtain a ligand concentration of 1 and then 5 nM. For each concentration, the uptake curves were measured for 120 min. Subsequently, the ^{57}Co-labeled DOTA-$Z_{EGFR:2377}$-containing medium was removed, fresh media (3 ml) was added to the dish, and the dissociation curve was recorded for 11 h. Two runs were performed at room temperature. The calculation of equilibrium dissociation constant was performed using TracerDrawer software (Ridgeview Instruments AB, Vänge, Sweden).

In vivo studies. All animal experiments were planned and performed in accordance with the Swedish national legislation on the protection of laboratory animals and the study plans were approved by the Ethics Committee for Animal Research in Uppsala. Euthanasia was performed by intraperitoneal injection of a ketamine-xylazine (Ketalar-Rompun) solution (200 mg/kg ketamine/Ketalar and 20 mg/kg xylazine/Rompun), and all efforts were made to minimize suffering. Female outbred BALB/c nu/nu mice (6 weeks of age) were purchased from Taconic M&B (Ry, Denmark). The animals (n=25) were housed at 23˚C, 45% humidity, 12-h light/dark cycle, food and water *ad libitum*. Prior to implantation the mice were quarantined for 1 week. At the time of experiment the average animal weight was 19±1 g. EGFR-expressing xenografts were established by subcutaneous injection of ~1x10^7 DU-145 cells/mouse. The tumors were grown for 8 days before the experiment (in Matrigel, BD Biosciences) and the average tumor weight was 0.13±0.08 g. Before the experiments the animals were randomized into groups of four.

The mice were intravenously injected with 30 kBq of radiolabeled conjugate per mouse in 100 μl PBS with 35 μg/mouse (one group) or 10 μg/mouse (three groups). The protein dose was adjusted by the addition of non-labeled DOTA-$Z_{EGFR:2377}$. The animals were sacrificed at 3 h pi (10- and 35-μg groups) and 7 and 24 h pi (10-μg groups). Blood, tumors and organ samples were collected and weighed, and their radioactivity was measured. Tissue uptake was calculated as the percent of injected dose per gram (% ID/g).

To verify specificity of *in vivo* targeting, a group of six mice was pre-injected with an excess amount of anti-EGFR monoclonal antibody cetuximab (5 mg/ml; cat. no. 64293; Merk KGaA, Darmstadt, Germany) 24 h prior to the injection of 10 μg (30 kBq) of ^{57}Co-DOTA-$Z_{EGFR:2377}$. The animals were sacrificed at 3 h pi. Cetuximab does not cross-react with murine EGFR, therefore only blood and tumors were collected for the blocking group.

Whole body scans of the subjects were performed using the Triumph™ Trimodality system (Gamma Medica, Inc., Salem, NH, USA), an integrated microSPECT/PET/CT platform. The mice bearing DU-145 xenografts were euthanized by CO_2 asphyxiation at 3, 7, and 24 h pi of 10 μg (4 MBq) ^{57}Co-DOTA-$Z_{EGFR:2377}$. The computed tomography (CT) acquisition was carried out at the following parameters: Field of view (FOV), 80 mm; magnification, 1.48; one projection and 512 frames for 2.13 min. SPECT acquisition was performed

at the following parameters: FOV, 80 mm; 75A10 collimators (5 pinhole); 64 projections, 2 h scan time. CT raw files were reconstructed by Filter Back Projection (FBP). SPECT raw data was reconstructed by the FLEX^{TM} SPECT software, which uses an ordered Subset Expectation Maximization (OSEM) iterative reconstruction algorithm. SPECT and CT data were fused and analyzed using PMOD v3.508 (PMOD Technologies Ltd., Zurich, Switzerland).

Statistical analysis. Data were assessed either by one-way ANOVA with Dunnett or with Bonferroni correction for multiple comparisons using GraphPad Prism 7.03 (GraphPad Software, Inc., La Jolla, CA, USA) in order to determine significant differences (P<0.05).

Results

Labeling with ^{57}Co under the selected conditions provided an average yield of 95±5%. After purification using disposable NAP-5 size-exclusion columns, the radiochemical purity was 100%.

In vitro cell studies. The results of binding specificity tests are presented in Fig. 1. Pre-saturation of EGFR with a large molar excess of non-labeled affibody molecules or EGFR-targeting mAb cetuximab resulted in a significantly reduced cell-associated radioactivity after 2 h incubation (n=3, P<0.05). On the contrary, the non-relevant mAb bevacizumab (anti-VEGF) did not influence the binding of the radioconjugate to cells. This finding indicated EGFR-mediated binding of ^{57}Co-DOTA-$Z_{EGFR:2377}$ to DU-145 cells.

Data concerning cellular processing of ^{57}Co-DOTA-$Z_{EGFR:2377}$ are presented in Fig. 2A. Cell-associated radioactivity increased continuously over time, while the contribution of internalized radioactivity was low, with <12% of total cell-associated radioactivity internalized after 24 h. The cellular retention of ^{57}Co-DOTA-$Z_{EGFR:2377}$ was also studied at various time-points (Fig. 2B). After an initial rapid dissociation phase (up to 2 h), the cell-associated radioactivity plateaued at 40% of initially bound radioactivity. The fraction of internalized radioactivity was low, similar to the previous experiment.

The binding affinity of ^{57}Co-DOTA-$Z_{EGFR:2377}$ to DU-145 cells was assessed in real-time. The evaluation of the binding kinetics revealed that the interaction did not follow a 1:1 Langmuir adsorption model. A superior fitting was obtained for the 1:2 model, suggesting two independent interactions with different kinetic parameters (Fig. 3A). The two processes occured simultaneously and consisted of a dominating high affinity interaction (79 pM, 66%) and a minor lower affinity interaction (3.7 nM, 17%) (Fig. 3B).

In vivo studies. Data concerning the biodistribution of ^{57}Co-DOTA-$Z_{EGFR:2377}$ in BALB/c nu/nu mice bearing DU-145 PCa xenografts are presented in Table I. In the first experiment, the biodistribution was compared at 3 h after injection of 35 and 10 μg of radiolabeled protein, respectively. A significant, dose-dependent difference in the accumulation of radioactivity in tumors and normal organs was observed. The concentration of radioactivity in blood and most normal organs (except for the spleen and muscles) was significantly higher in the 10-μg group (n=4, P<0.05). Tumor uptake was also 2-fold higher in the group of mice injected with 10 μg of ^{57}Co-DOTA-$Z_{EGFR:2377}$ (2.1±0.1% IA/g), compared to the 35-μg group (1.1±0.1% IA/g). Tumor-to-non-tumor ratios were similar in both groups. The high uptake in kidneys indicated that ^{57}Co-DOTA-$Z_{EGFR:2377}$ was cleared by glomerular filtration with subsequent tubular re-absorption.

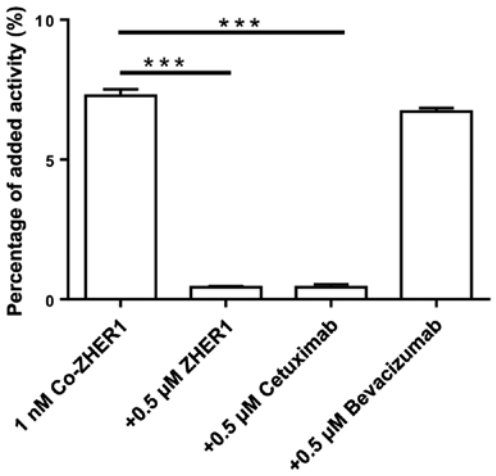

Figure 1. *In vitro* specificity test for ^{57}Co-DOTA-$Z_{EGFR:2377}$ on DU-145 cells. Blocked dishes were pre-saturated with molar excess of non-labeled peptide (0.5 μM), Cetuximab (0.5 μM) and Bevacizumab (0.5 μM) 10 min prior to the addition of 1 nM radiolabeled compound with 500 fold molar excess. The cell-associated radioactivity was calculated as a percentage of the total added radioactivity (mean values of three dishes ± SD). Asterisks mark significant differences (n=3, ***P<0.05). Data were assessed by one-way ANOVA with Dunnett correction for multiple comparisons.

Specificity of EGFR-targeting *in vivo* was assessed by pre-saturation of receptors with non-labeled monoclonal antibody cetuximab. The tumor uptake in the blocked group of mice was significantly reduced (P<0.05) compared to the control group. No significant difference was found in the radioactivity uptake in blood (Table I).

Data on the biodistribution of ^{57}Co-DOTA-$Z_{EGFR:2377}$ over time are presented in Table I. In this experiment, two additional groups of mice were injected with 10 μg and the animals were sacrificed at 7 and 24 h pi. There was no significant release of radioactivity from the tumors between 3 and 7 h pi, but radioactivity uptake in tumors dropped 2-fold at 24 h pi. The clearance from blood and normal organs was also relatively slow, and with the exception of lungs, spleen and colon, there was no noticeable decrease in the radioactivity concentration between 3 and 7 h pi. However, radioactivity uptake in normal organs decreased 3-fold at 24 h pi which was rapider than in tumors. As a result, tumor-to-non-tumor ratios were not significantly improved between 3 and 7 h pi, but significantly increased at 24 h pi (n=4, P<0.05) (Fig. 4).

MicroSPECT scans were acquired at 3, 7, and 24 h after the intravenous administration of 10 μg (4 MBq) ^{57}Co-DOTA-$Z_{EGFR:2377}$ to BALB/c nu/nu mice bearing subcutaneous DU-145 xenografts (Fig. 5). SPECT/CT images confirmed the capacity of ^{57}Co-DOTA-$Z_{EGFR:2377}$ to visualize EGFR expression. The highest uptake of radioactivity was observed in the kidneys, followed by the liver, concordant with the biodistribution results. The microSPECT experiment confirmed that imaging of EGFR expression in PCa is possible.

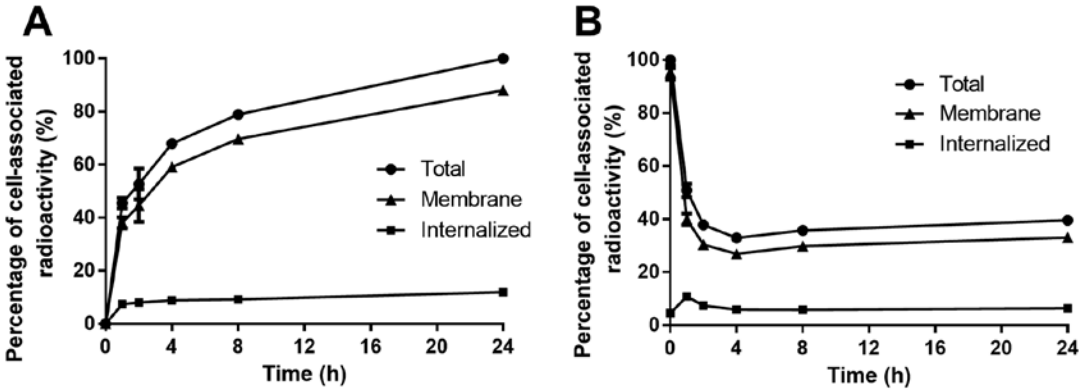

Figure 2. Cellular processing of ^{57}Co-DOTA-$Z_{EGFR:2377}$ by DU-145 cells during (A) continuous incubation with 1.5 nM of ^{57}Co-DOTA-$Z_{EGFR:2377}$ and (B) after interrupted incubation with 1.5 nM of ^{57}Co-DOTA-$Z_{EGFR:2377}$. Data are presented as the means ± SD of three culture dishes. Error bars may not be visible because they are smaller than point symbols.

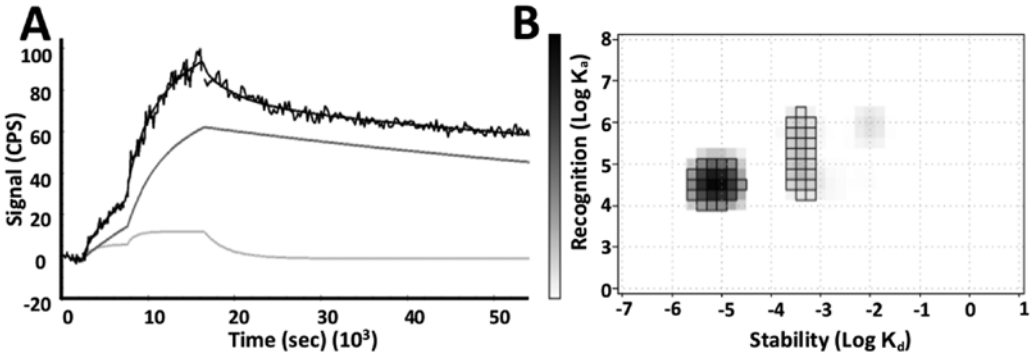

Figure 3. (A) LigandTracer sensorgram and fitted binding curve (black) of ^{57}Co-DOTA-$Z_{EGFR:2377}$ interaction with EGFR-expressing DU-145 cells at room temperature. Uptake curves were recorded at 1 and 5 nM. The data were fitted to a one-to-two interaction model and represent the combination of two distinct interactions: A dominating high affinity interaction 0.08 nM (dark grey) and a minor interaction of lower affinity of 3.7 nM (light grey). (B) Interaction map: The simultaneous interactions are observed as distinct processes in the map. The grey scale reflects the contribution of each interaction (66% for 0.08 nM, 17% for 3.7 nM). Darker areas corresponded to larger contributions.

Table I. Biodistribution of ^{57}Co-DOTA-$Z_{EGFR:2377}$ after injection in BALB/c nu/nu mice bearing DU-145 xenografts.

	35 μg	10 μg		
	3 h	3 h	7 h	24 h
Blood	0.73±0.08[a]	1.8±0.6 (2.0±0.8)	1.3±0.2	0.30±0.04[b,c]
Saliv. glands	0.62±0.04	1.23±0.08	1.1±0.2	0.44±0.05[b,c]
Lung	0.77±0.06	1.9±0.2	1.3±0.1[b]	0.44±0.05[b,c]
Liver	4.8±0.5	7±2	5.3±1.7	3.1±0.5[b]
Spleen	1.1±0.2	1.0±0.1	0.69±0.05[b]	0.8±0.1
Small int.	0.69±0.04[a]	1.3±0.2	1.0±0.2	0.45±0.02[b,c]
Colon	0.64±0.09[a]	1.34±0.09	1.10±0.09[b]	0.48±0.09[b,c]
Kidney	319±17	300±30	278±27	247±29
Tumor	1.1±0.1[a]	2.1±0.5[d] (1.3±0.2)	1.8±0.3	1.0±0.2[b]
Muscle	0.4±0.4	0.35±0.06	0.26±0.05	0.15±0.04[b]
Bone	0.40±0.07[a]	0.7±0.2	0.57±0.09	0.26±0.03[b,c]

Data represent the percentage of injected dose per gram tissue (% ID/g) and are expressed as the mean value ± SD (n=4). Data within parenthesis were collected from mice pre-injected with an excess amount of the anti-EGFR monoclonal antibody cetuximab. Since cetuximab does not cross-react with murine EGFR, only blood and tumor uptake were evaluated. Data were assessed either by one-way ANOVA with Dunnett ([e]) or Bonferroni ([f]) correction for multiple comparisons in order to determine significant differences (P<0.05). [a]Value was significantly lower than for 10 μg[e]; [b]value was significantly lower than for 3 h, 10 μg[f]; [c]value was significantly lower than for 7 h, 10 μg[f]; [d]value was significantly higher than for mice pre-injected with an excess amount of cetuximab[e]. EGFR, epidermal growth factor receptor.

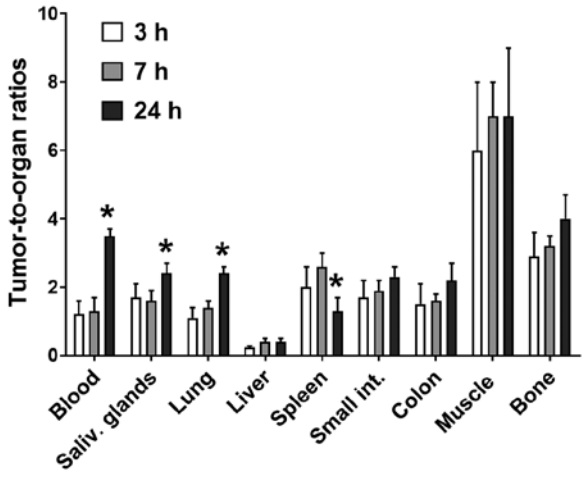

Figure 4. Tumor-to-organ ratios for ^{57}Co-DOTA-$Z_{EGFR:2377}$ after injection of 10 μg in BALB/C nu/nu mice bearing DU-145 xenografts. Data are presented as the mean value ± SD. Asterisks mark organs where the tumor-to-organ ratio significantly differed between 7 and 24 h pi (n=4, P<0.05). Data were assessed by one-way ANOVA with Bonferroni correction for multiple comparisons.

Discussion

EGFR is significantly upregulated in advanced stages of PCa and is associated with a high risk of recurrence, progression towards androgen independence and metastasis (8). Therefore, EGFR has emerged as a promising target for second-line therapy of disseminated PCa. Such therapies include neutralization of EGFR by mAb that prevent binding to its ligands and the subsequent activation of downstream signaling pathways and TKI that compete with the ATP binding site of the catalytic domain of tyrosine kinases (39,40). However, the use of anti-EGFR mAb cetuximab for treatment of unselected patients exhibited a limited success if any (41,42). Moreover, adding cetuximab to other therapeutics often aggravated the side-effects. Both studies claimed the necessity of predictive biomarkers for EGFR-targeted therapy of PCa. Fleming *et al* demonstrated in a post hoc analysis that appearance of a rash could be a pharmacodynamics biomarker for response enabling selection of tailored dosing of cetuximab (42). A further study demonstrated that EGFR overexpression was correlated with the response of PCa to cetuximab treatment (43). A probe enabling imaging of EGFR expression in PCa metastases before treatment and data concerning receptor occupancy during treatment would provide important predictive and pharmacodynamic information and would facilitate the use of cetuximab and TKI for the treatment of PCa.

Comparison of data from our previous studies (32-34) demonstrated that ^{57}Co-DOTA-$Z_{EGFR:2377}$ provided better contrast of EGFR imaging than ^{89}Zr-cetuximab and $Z_{EGFR:2377}$ variants labeled with ^{111}In, ^{68}Ga or ^{89}Zr. Notably, ^{57}Co-$Z_{EGFR:2377}$ binds to the same epitope as cetuximab as seen in the *in vitro* binding specificity assay. In this experiment, the uptake of ^{57}Co-$Z_{EGFR:2377}$ on EGFR-expressing DU-145 cells was successfully blocked by the addition of excess cetuximab (Fig. 1). Binding specificity was further confirmed *in vivo* in mice bearing DU-145 xenografts. The uptake of ^{57}Co-$Z_{EGFR:2377}$ in tumors was significantly lower in mice pre-injected with an excess amount of cetuximab, while the blood-born radioactivity was similar (Table I). These experiments indicated that radiocobalt-labeled $Z_{EGFR:2377}$ could be used for monitoring receptor occupancy during cetuximab therapy. The significant reduction of ^{57}Co-DOTA-$Z_{EGFR:2377}$ tumor uptake in a post-treatment scan compared to a baseline image would indicate that EGFR in the lesion was blocked sufficiently.

Data concerning cellular (Fig. 2) processing of ^{57}Co-DOTA-$Z_{EGFR:2377}$ were in agreement with the data for A431 cells (37). In both cases, the internalized fraction was unexpectedly low for a radiometal label (below 15% after 24 h). For comparison, the internalized fraction reached 30% for the same conjugate radiolabeled with indium-111 (37). The study of radioactivity retention after interrupted incubation also revealed a low internalized fraction that did not increase with time (Fig. 2). Collectively, this may indicate lower residualizing properties of cobalt-containing radiocatabolites that could lead to lower retention of labels in tumors *in vivo* over time.

The presence of two types of binding sites characterized by different affinities was found when evaluating the binding kinetics of ^{57}Co-DOTA-$Z_{EGFR:2377}$ to EGFR-expressing DU-145 cells. The data indicated the existence of two populations of EGFR in DU-145 cells: The major one with picomolar affinity and another one with low nanomolar affinity. This finding was consistent with previous results when binding of natural ligand EGF to EGFR was studied (38) and was revealed to vary depending on culturing conditions (44,45). A possible explanation for the two types of interactions is receptor homo- and heterodimerization, which can result in different accessibility of binding sites. It should to be noted that both interactions were strong (0.08 and 3.7 nM), with the strongest interaction predominant.

One of the main obstacles for imaging of EGFR expression in tumors is an appreciable EGFR expression in a number of normal tissues, particularly in liver hepatocytes. Liver is a large well-perfused organ. The injection of an insufficient amount of e.g. anti-EGFR antibody may result in its nearly complete trapping in liver (46). Clinical studies have demonstrated, however, that it is possible to adjust the dose of the anti-EGFR antibody to saturate EGFR in liver and provide release of radiolabeled antibody into circulation (23). We have also shown in preclinical studies that it is possible to partially saturate murine EGFR in liver with ^{111}In-DOTA-$Z_{EGFR:2377}$ without saturating receptors in xenografts (32). The optimal protein dose, 35 μg, was also used in the previous study with ^{57}Co-DOTA-$Z_{EGFR:2377}$ (33).

However, these initial studies utilized the A431 cell line, having EGFR expression of ~2x10^6 receptors/cell. The expression level of EGFR in PCa is appreciably lower (Human Protein Atlas http://www.proteinatlas.org/). For example, the DU-145 cell line has an EGFR expression of 2x10^5 receptors/cell, i.e. one order of magnitude lower than A431 cells. The average tumor weight at the time of the experiment was 0.13±0.08 g corresponding to lesions of 4 mm in diameter. The spatial resolution of modern clinical PET cameras is 6-10 mm and radioactivity concentration in any objects below this size will be underestimated due to partial volume effect. Taking this in account, the tumors in our study were relatively small from a clinical perspective. The *in vivo* data revealed a pronounced

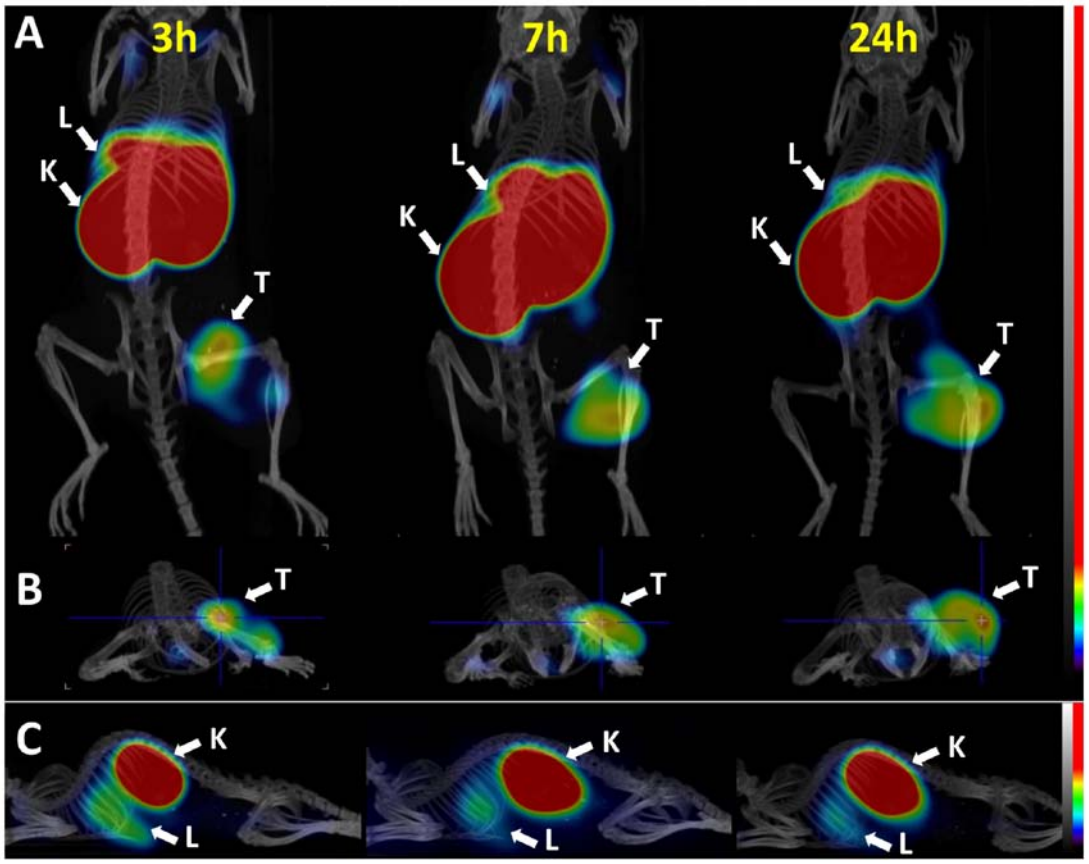

Figure 5. (A) Coronal, (B) Axial, and (C) Sagittal images of EGFR expression in DU-145 xenografted BALB/c nu/nu mice. The animals were injected with 10 μg of ^{57}Co-DOTA-$Z_{EGFR:2377}$ (4 MBq) and euthanized at 3, 7, and 24 h after injection. K, kidney; L, liver; T, tumor.

influence of injected dose on the biodistribution profile of ^{57}Co-DOTA-$Z_{EGFR:2377}$. We compared the biodistribution and tumor uptake after the injection of 35 μg [dose found optimal for high EGFR expression xenografts A431 (32,33)] and 10 μg of radiolabeled conjugate at 3 h pi. A detailed dose-dependent uptake of anti-EGFR affibody molecules in normal organs was previously studied in detail by Tolmachev *et al* (32), creating the rationale for the choice of protein doses tested in the present study.

Our reasoning was that a high protein dose could lead to saturation of EGFR in tumors with low expression level in the same manner as in normal organs with EGFR expression, such as salivary glands and intestine walls. Decreasing the protein dose resulted in a significant increase of uptake in tumors as well as in most studied organs including blood. The same phenomenon was also observed for ^{111}In-DOTA-$Z_{EGFR:2377}$ and ^{111}In-DOTA-$Z_{EGFR:1907}$ studied in high EGFR-expressing A431 xenografts (32,46). The elevated blood radioactivity may be attributed to the dissociation of non-internalized radioconjugates from EGFR-expressing organs followed by re-entrance in blood circulation. In the group of mice injected with 35 μg ^{57}Co-DOTA-$Z_{EGFR:2377}$, the binding sites were partially saturated with non-labeled compound, which lead to a reduction of uptake in tumors and EGFR-expressing organs (liver, salivary glands, lungs) and lower blood-born radioactivity. However, in the low EGFR-expressing xenografts used in the present study, the decrease in protein dose resulted in a significant 2-fold increase in radioactivity uptake in tumors (n=4, $P<0.05$).

The higher tumor uptake would increase the sensitivity of imaging of lesions with low receptor expression, such as EGFR in PCa. Therefore, the injected dose of 10 μg was used for measuring the biodistribution over time. The time-points assessed in the present study were chosen to be clinically relevant: 3 and 7 h pi correspond to same-day imaging while 24 h pi corresponds to next-day imaging.

Due to the slow clearance of radioactivity from blood and normal organs, the tumor-to-organ ratios were not significantly improved between 3 and 7 h pi. At the later time-point of 24 h pi, the faster clearance from normal tissues compared to tumors resulted in significantly higher tumor-to-organ ratios that enhanced imaging contrast. In contrast to the results obtained for ^{57}Co-DOTA-$Z_{EGFR:2377}$ in a high EGFR-expressing model (33), the conjugate did not provide positive contrast towards the liver. However, this is not critical for PCa where liver metastases are not common. Still, the uptake in tumors after the injection of 10 μg ^{57}Co-DOTA-$Z_{EGFR:2377}$ exceeded the uptake in all other studied organs with the exception of the liver and kidneys. For organs clinically relevant for the detection of PCa lesions, tumor-to-organ ratios at 24 h pi were 2.2±0.5 for the colon, 7±2 for muscle, and 4.0±0.7 for bones. Therefore ^{57}Co-DOTA-$Z_{EGFR:2377}$ was successful in visualizing the EGFR-expression in PCa as early as 3 h pi and imaging contrast improved with time (Fig. 4). Previously it was demonstrated that a single-dose injection of anti-EGFR affibody molecule produced no pathological evidence of toxicity in rats at a dose level of 24,490 μg/kg (corresponding to a 1,000x equivalent

human microdose level) (47). Dosimetry estimated using clinical data for the anti-HER2 affibody molecule, a tracer with a comparable kidney uptake, revealed that the absorbed dose to kidneys and liver, after a 100-MBq administration (Ga-68), would be ~40 and 15 mGy, respectively, which is less than the maximum allowed absorbed dose of 50 mGy to a single organ in a healthy adult research subject. The administration of ~200 MBq would give an effective dose in the range of 5-6 mSv (lower than for typical ^{18}F-FDG PET examinations, which often give effective doses of around 7 mSv (48). We may expect that for the anti-EGFR imaging probe the absorbed doses for kidneys should be similar and the absorbed dose for liver should be somewhat higher than that for the anti-HER2 imaging probe.

In conclusion, radiocobalt-labeled DOTA-$Z_{EGFR:2377}$ allowed the successful visualization of EGFR *in vivo* in a PCa pre-clinical model and could be used for monitoring of receptor occupancy during cetuximab therapy. The present study also emphasized the importance of finding optimal protein dosing for tumors with low EGFR expression in order to ensure a higher sensitivity in clinical imaging.

Acknowledgements

Not applicable.

Funding

The present study was supported by the Swedish Cancer Society [grants CAN 2017/649 (JL), CAN2013/586 and CAN 2016/463 (SS), CAN2014/474, CAN 2017/425 (AO), and CAN2015/350 (VT)], the Swedish Research Council [grants 621-2012-5236 (SS), 2015-02509 (AO), and 2015-02353 (VT)], the Swedish Agency for Innovation VINNOVA [grants 2016-04060 (AO) and 2017-02015 (SS, JL)] and the Wallenberg Center for Protein Technology (SS, JL). The molecular imaging work in this publication was supported by the Wallenberg infrastructure for PET-MRI (WIPPET) at SciLifeLab Pilot Facility for Preclinical PET-MRI, a Swedish nationally available imaging platform at Uppsala University, Sweden, financed by the Knut and Alice Wallenberg Foundation (SPECT/CT).

Availability of data and materials

The datasets used during the present study are available from the corresponding author upon reasonable request.

Authors' contributions

BM participated in the labeling of proteins, the *in vitro* and *in vivo* characterization, the data acquisition, data interpretation and drafted the first version of manuscript; KGA and JG performed the production and the following biochemical, biophysical and *in vitro* characterization of conjugate; EL participated in the labeling of proteins, the *in vitro* and *in vivo* characterization, the data acquisition and data interpretation; MR participated in the *in vivo* characterization and the data acquisition; VT and AO participated in the molecular and study design, in the *in vivo* characterization, the data acquisition, data interpretation, drafted the relevant parts of the manuscript and critically revised the manuscript; SS and JL participated in the molecular and study design, the data acquisition, data interpretation and critically revised the manuscript. All authors read and approved the manuscript and agree to be accountable for all aspects of the research in ensuring that the accuracy or integrity of any part of the work are appropriately investigated and resolved.

Ethics approval and consent to participate

All animal experiments were planned and performed in accordance with the Swedish national legislation on the protection of laboratory animals and the study plans were approved by the Ethics Committee for Animal Research in Uppsala.

Patient consent for publication

Not applicable.

Competing interests

The authors declare that they have no competing interests.

References

1. Huggins C and Hodges CV: Studies on prostate cancer. I. The effect of castration, of estrogen and of androgen injection on serum phosphatases in metastatic carcinoma of the prostate. CA Cancer J Clin 22: 232-240, 1972.
2. Pienta KJ and Bradley F: Mechanisms underlying the development of androgen-independent PC. Clin Cancer Res 12: 1665-1671, 2006.
3. Hoffman P and Djavan B: Androgen deprivation therapy. Rev Urol 10: 305-306, 2008.
4. Yagoda A and Petrylak D: Cytotoxic chemotherapy for advanced hormone-resistant prostate cancer. Cancer 71 (Suppl 3): S1098-S1109, 1993.
5. Raghavan D, Koczwara B and Javle M: Evolving strategies of cytotoxic chemotherapy for advanced prostate cancer. Eur J Cancer 33: 566-574, 1997.
6. Mimeault M and Batra SK: Recent advances on multiple tumorigenic cascades involved in prostatic cancer progression and targeting therapies. Carcinogenesis 27: 1-22, 2006.
7. Djakiew D: Dysregulated expression of growth factors and their receptors in the development of prostate cancer. Prostate 42: 150-160, 2000.
8. Hernes E, Fosså SD, Berner AA, Otnes B and Nesland JM: Expression of the epidermal growth factor receptor family in prostate carcinoma before and during androgen-independence. Br J Cancer 90: 449-454, 2004.
9. Schlomm T, Kirstein P, Iwers L, Daniel B, Steuber T, Walz J, Chun FH, Haese A, Kollermann J, Graefen M, *et al*: Clinical significance of epidermal growth factor receptor protein overexpression and gene copy number gains in prostate cancer. Clin Cancer Res 13: 6579-6584, 2007.
10. Shaw G and Prowse DM: Inhibition of androgen-independent PC cell growth is enhanced by combination therapy targeting Hedgehog and ErbB signaling. Cancer Cell Int 8: 3, 2008.
11. Marmor MD, Skaria KB and Yarden Y: Signal transduction and oncogenesis by ErbB/HER receptors. Int J Radiat Oncol Biol Phys 58: 903-913, 2004.
12. Oda K, Matsuoka Y, Funahashi A and Kitano H: A comprehensive pathway map of epidermal growth factor receptor signalling. Mol Syst Biol 1: 2005.0010, 2005.
13. Baselga J: The EGFR as a target for anticancer therapy-focus on cetuximab. Eur J Cancer 37 (Suppl 4): S16-S22, 2001.
14. Herbst RS, Kim ES and Harari PM: IMC-C225, an anti-epidermal growth factor receptor monoclonal antibody, for treatment of head and neck cancer. Expert Opin Biol Ther 1: 719-732, 2001.
15. Bonomi P: Erlotinib: A new therapeutic approach for non-small cell lung cancer. Expert Opin Investig Drugs 12: 1395-1401, 2003.

16. Herbst RS: Erlotinib (Tarceva): An update on the clinical trial program. Semin Oncol 30 (3 Suppl 7): S34-S46, 2003.
17. Fukuoka M, Yano S, Giaccone G, Tamura T, Nakagawa K, Douillard JY, Nishiwaki Y, Vansteenkiste J, Kudoh S, Rischin D, *et al*: Multi-institutional randomized phase II trial of gefitinib for previously treated patients with advanced non-small-cell lung cancer (The IDEAL 1 Trial). J Clin Oncol 21: 2237-2246, 2003.
18. Ranson M, Hammond LA, Ferry D, Kris M, Tullo A, Murray PI, Miller V, Averbuch S, Ochs J, Morris C, *et al*: A selective oral epidermal growth factor receptor-tyrosine kinase inhibitor, is well tolerated and active in patients with solid, malignant tumors: Results of a phase I trial. J Clin Oncol 2: 2240-2250, 2002.
19. Guérin O, Fischel JL, Ferrero JM, Bozec A and Milano G: EGFR targeting in hormone-refractory prostate cancer: Current appraisal and prospects for treatment. Pharmaceuticals (Basel) 3: 2238-2247, 2010.
20. Vignot S, Besse B, André F, Spano JP and Soria JC: Discrepancies between primary tumor and metastasis: A literature review on clinically established biomarkers. Crit Rev Oncol Hematol 84: 301-313, 2012.
21. Cuartero-Plaza A, Martínez-Miralles E, Rosell R, Vadell-Nadal C, Farré M and Real FX: Radiolocalization of squamous lung carcinoma with 131I-labeled epidermal growth factor. Clin Cancer Res 2: 13-20, 1996.
22. Goldenberg A, Masui H, Divgi C, Kamrath H, Pentlow K and Mendelsohn J: Imaging of human tumor xenografts with an indium-111-labeled anti-epidermal growth factor receptor monoclonal antibody. J Natl Cancer Inst 81: 1616-1625, 1989.
23. Divgi CR, Welt S, Kris M, Real FX, Yeh SD, Gralla R, Merchant B, Schweighart S, Unger M, Larson SM, *et al*: Phase I and imaging trial of indium 111-labeled anti-epidermal growth factor receptor monoclonal antibody 225 in patients with squamous cell lung carcinoma. J Natl Cancer Inst 83: 97-104, 1991.
24. Cai W, Chen K, He L, Cao Q, Koong A and Chen X: Quantitative PET of EGFR expression in xenograft-bearing mice using ^{64}Cu-labeled cetuximab, a chimeric anti-EGFR monoclonal antibody. Eur J Nucl Med Mol Imaging 34: 850-858, 2007.
25. Ping Li W, Meyer LA, Capretto DA, Sherman CD and Anderson CJ: Receptor-binding, biodistribution, and metabolism studies of ^{64}Cu-DOTA-cetuximab, a PET-imaging agent for epidermal growth-factor receptor-positive tumors. Cancer Biother Radiopharm 23: 158-171, 2008.
26. Nayak TK, Garmestani K, Baidoo KE, Milenic DE and Brechbiel MW: Preparation, biological evaluation, and pharmacokinetics of the human anti-HER1 monoclonal antibody panitumumab labeled with 86Y for quantitative PET of carcinoma. J Nucl Med 51: 942-950, 2010.
27. Nayak TK, Garmestani K, Milenic DE and Brechbiel MW: PET and MRI of metastatic peritoneal and pulmonary colorectal cancer in mice with human epidermal growth factor receptor 1-targeted ^{89}Zr-labeled panitumumab. J Nucl Med 53: 113-120, 2012.
28. Chang AJ, De Silva RA and Lapi SE: Development and characterization of ^{89}Zr-labeled panitumumab for immuno-positron emission tomographic imaging of the epidermal growth factor receptor. Mol Imaging 12: 17-27, 2013.
29. Ahlgren S and Tolmachev V: Radionuclide molecular imaging using Affibody molecules. Curr Pharm Biotechnol 11: 581-589, 2010.
30. Sörensen J, Sandberg D, Sandström M, Wennborg A, Feldwisch J, Tolmachev V, Åström G, Lubberink M, Garske-Román U, Carlsson J and Lindman H: First-in-human molecular imaging of HER2 expression in breast cancer metastases using the ^{111}In-ABY-025 affibody molecule. J Nucl Med 55: 730-735, 2014.
31. Sörensen J, Velikyan I, Sandberg D, Wennborg A, Feldwisch J, Tolmachev V, Orlova A, Sandström M, Lubberink M, Olofsson H, *et al*: Measuring HER2-receptor expression in metastatic breast cancer using [^{68}Ga]ABY-025 affibody PET/CT. Theranostics 6: 262-271, 2016.
32. Tolmachev V, Rosik D, Wållberg H, Sjöberg A, Sandström M, Hansson M, Wennborg A and Orlova A: Imaging of EGFR expression in murine xenografts using site-specifically labelled anti-EGFR ^{111}In-DOTA-ZEGFR:2377 Affibody molecule: Aspect of the injected tracer amount. Eur J Nucl Med Mol Imaging 37: 613-622, 2010.
33. Garousi J, Andersson KG, Dam JH, Olsen BB, Orlova A, Buijs J, Ståhl S, Löfblom J, Thisgaard H and Tolmachev V: The use of radiocobalt as a label improves imaging of EGFR using DOTA-conjugated Affibody molecule. Sci Rep 7: 5961, 2017.
34. Garousi J, Andersson KG, Mitran B, Pichl ML, Ståhl S, Orlova A, Löfblom J and Tolmachev V: PET imaging of epidermal growth factor receptor expression in tumours using ^{89}Zr-labelled ZEGFR:2377 affibody molecules. Int J Oncol 48: 1325-1332, 2016.
35. Yang D, Kuan CT, Payne J, Kihara A, Murray A, Wang LM, Alimandi M, Pierce JH, Pastan I and Lippman ME: Recombinant heregulin-Pseudomonas exotoxin fusion proteins: Interactions with the heregulin receptors and antitumor activity in vivo. Clin Cancer Res 4: 993-1004, 1998.
36. Mitran B, Thisgaard H, Rosenström U, Dam JH, Larhed M, Tolmachev V, and Orlova A: High contrast PET imaging of GRPR expression in prostate cancer using cobalt-labeled Bombesin antagonist RM26. Contrast Media Mol Imaging 2017: 6873684, 2017
37. Malmberg J, Tolmachev V and Orlova A: Imaging agents for in vivo molecular profiling of disseminated prostate cancer-targeting EGFR receptors in prostate cancer: Comparison of cellular processing of [^{111}In]-labeled affibody molecule Z(EGFR:2377) and cetuximab. Int J Oncol 38: 1137-1143, 2011.
38. Björkelund H, Gedda L and Andersson K: Comparing the epidermal growth factor interaction with four different cell lines: Intriguing effects imply strong dependency of cellular context. PLoS One 6: e16536, 2011.
39. Rocha-Lima CM, Soares HP, Raez LE and Singal R: EGFR targeting of solid tumors. Cancer Control 14: 295-304, 2007.
40. Henson E, Chen Y and Gibson S: EGFR family members' regulation of autophagy is at a crossroads of cell survival and death in cancer. Cancers (Basel) 9: E27, 2017.
41. Slovin SF, Kelly WK, Wilton A, Kattan M, Myskowski P, Mendelsohn J and Scher HI: Anti-epidermal growth factor receptor monoclonal antibody cetuximab plus Doxorubicin in the treatment of metastatic castration-resistant prostate cancer. Clin Genitourin Cancer 7: E77-E82, 2009.
42. Fleming MT, Sonpavde G, Kolodziej M, Awasthi S, Hutson TE, Martincic D, Rastogi A, Rousey SR, Weinstein RE, Galsky MD, *et al*: Association of rash with outcomes in a randomized phase II trial evaluating cetuximab in combination with mitoxantrone plus prednisone after docetaxel for metastatic castration-resistant prostate cancer. Clin Genitourin Cancer 10: 6-14, 2012.
43. Cathomas R, Rothermundt C, Klingbiel D, Bubendorf L, Jaggi R, Betticher DC, Brauchli P, Cotting D, Droege C, Winterhalder R, *et al*: Efficacy of cetuximab in metastatic castration-resistant prostate cancer might depend on EGFR and PTEN expression: Results from a phase II trial (SAKK 08/07). Clin Cancer Res 18: 6049-6057, 2012.
44. Özcan F, Klein P, Lemmon MA, Lax I and Schlessinger J: On the nature of low- and high-affinity EGF receptors on living cells. Proc Natl Acad Sci USA 103: 5735-5740, 2006.
45. Björkelund H, Gedda L, Malmqvist M and Andersson K: Resolving the EGF-EGFR interaction characteristics through a multiple-temperature, multiple-inhibitor, real-time interaction analysis approach. Mol Clin Oncol 1: 343-352, 2013.
46. Tolmachev V, Friedman M, Sandström M, Eriksson TL, Rosik D, Hodik M, Ståhl S, Frejd FY and Orlova A: Affibody molecules for epidermal growth factor receptor targeting in vivo: Aspects of dimerization and labeling chemistry. J Nucl Med 50: 274-283, 2009.
47. Samkoe KS, Gunn JR, Marra K, Hull SM, Moodie KL, Feldwisch J, Strong TV, Draney DR, Hoopes PJ, Roberts DW, *et al*: Toxicity and pharmacokinetic profile for single-dose injection of ABY-029: A fluorescent anti-EGFR synthetic affibody molecule for human use. Mol Imaging Biol 19: 512-521, 2017.
48. Sandström M, Lindskog K, Velikyan I, Wennborg A, Feldwisch J, Sandberg D, Tolmachev V, Orlova A, Sörensen J, Carlsson J, *et al*: Biodistribution and radiation dosimetry of the Anti-HER2 affibody molecule ^{68}Ga-ABY-025 in breast cancer patients. J Nucl Med 57: 867-871, 2016.